

Safe Networked Robotics via Formal Verification

Sai Shankar Narasimhan, Sharachchandra Bhat, Sandeep P. Chinchali

Department of Electrical and Computer Engineering

The University of Texas at Austin

{nsaishankar, sharachchandra, sandeepc}@utexas.edu

Abstract—Autonomous robots must utilize rich sensory data to make safe control decisions. Often, compute-constrained robots require assistance from remote computation (“the cloud”) if they need to invoke compute-intensive Deep Neural Network perception or control models. Likewise, a robot can be remotely teleoperated by a human during risky scenarios. However, this assistance comes at the cost of a time delay due to network latency, resulting in stale/delayed observations being used in the cloud to compute the control commands for the present robot state. Such communication delays could potentially lead to the violation of essential safety properties, such as collision avoidance. This paper develops methods to ensure the safety of teleoperated robots with stochastic latency. To do so, we use tools from formal verification to construct a shield (i.e., run-time monitor) that provides a list of safe actions for any delayed sensory observation, given the expected and worst-case network latency. Our shield is *minimally intrusive* and enables networked robots to satisfy key safety constraints, expressed as temporal logic specifications, with high probability. Our approach gracefully improves a teleoperated robot’s safety vs. efficiency trade-off as a function of network latency, allowing us to quantify performance gains for WiFi or even future 5G networks. We demonstrate our approach on a real F1/10th autonomous vehicle that navigates in crowded indoor environments and transmits rich LiDAR sensory data over congested WiFi links.

I. INTRODUCTION

Today, we are seeing more applications of teleoperated robots, ranging from remote manipulation/surgery [13, 23, 8] to emergency take-over of autonomous vehicles [12]. Teleoperation is often used to collect rich demonstration data for imitation learning of manipulation policies [26, 27, 15] or even to control fleets of food delivery robots from command centers hundreds of miles away [1]. Network latency is a key concern for teleoperation since actuation based on delayed state information can lead to unsafe behavior.

Despite the rise of teleoperated robots, we lack formal guarantees on safe teleoperation over uncertain wireless networks. Today’s approaches for robotic safety range from reachability analysis [5] to synthesizing shields that restrict unsafe actions based on a formal safety specification [3]. However, there is little to no research that provides such rigorous safety analysis for teleoperation. This paper asks: *How do we characterize and ensure safe teleoperation over stochastic wireless networks?*

Our key insight is that teleoperation with stochastic network delays can be cast as a Markov Decision Process (MDP). We develop the intuition that there are two stochastic elements - the network latency/delay and the environment that includes

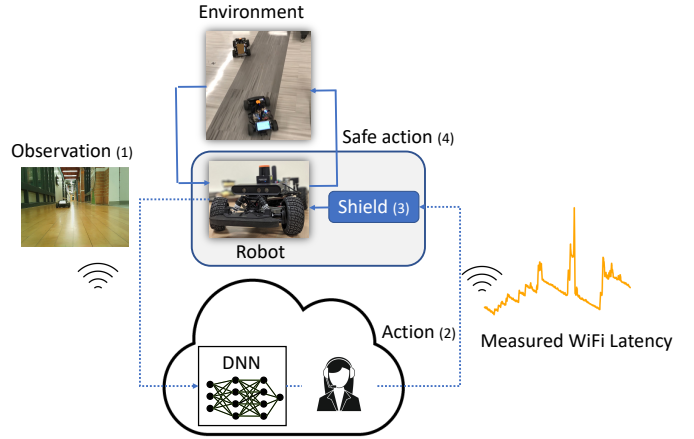


Fig. 1: **Safe Networked Control for Robotics:** A resource-constrained robot transfers sensor observations (RGB-D images / LIDAR point clouds) through a stochastic communication network. At the receiving end, a teleoperator or a control module takes the observation and generates the corresponding action. The action is filtered by the shield, which enforces a particular safety specification that the robot has to maintain. The filtered and “safe” action is then executed by the robot, which we test on a real hardware platform.

dynamic obstacles. As we are concerned with the safety of networked control systems, we need to consider all possible transitions for both the network delay and the environment, hence the MDP. Moreover, we can use expressive logical specifications, such as linear temporal logic (LTL) [11], to formally specify safety considerations, such as collision avoidance and reach-avoid behavior.

Fig. 1 shows our approach, which we test on a real F1/10th autonomous racecar [22] that is teleoperated over a heavily-congested wireless link. Our approach is extremely general – we can either have a remote human teleoperator or an automatic controller running in the cloud. For example, if our robot is limited by computing, memory, or power, it can offload the inference of a DNN perception model and deep reinforcement learning (RL) controller to the cloud. We can flexibly also run a model predictive controller (MPC) [6, 7] in the cloud. First, the robot sends a sensory observation, such as a video or a LiDAR point cloud, over WiFi to the cloud (Fig. 1, step 1). Then, the cloud uses the sensory observation to compute a control command, which is sent to the robot over a stochastic wireless link (step 2). Then, we implement a run-time shield on the robot, which disallows unsafe actions that violate a formal safety specification, using tools from

⁰These authors contributed equally to this work

formal verification (step 3) [4]. When placed on the robot, the shield has access to the current network latency. Shields are minimally intrusive, i.e., the shield overwrites the control only if it is deemed unsafe and could result in a safety violation. Finally, the robot implements the shielded action (step 4), which guarantees safe behavior given reasonable assumptions on network latency and a coarse model of other nearby agents’ behavior.

Shields, as implemented in [3], are very conservative. Thus, for networked control tasks where there is stochasticity in network latency and environment transitions, patching the teleoperation/“cloud” control commands with shields results in perfectly safe operation at the cost of task efficiency. Similar to [16], we implement probabilistic shields δ -shield that take into account the probabilistic transitions of network latency and the environment to ensure that the safety specifications are satisfied with high probability.

Statement of Contributions: Our contributions are:

- 1) We present the first work to synthesize a shield for networked control systems with stochastic latency for a general set of safety specifications. Our method can shield any off-the-shelf controller (RL or MPC) given bounds on the expected and worst-case latency.
- 2) Our approach gracefully improves a teleoperated robot’s safety vs. efficiency trade-off based on the latency statistics. This allows us to quantify performance gains for WiFi or even future 5G wireless networks.
- 3) We demonstrate our approach in simulation as well as on a pair of real F1/10th autonomous vehicles that must closely (and safely) follow each other in crowded indoor environments over congested wireless networks.

II. RELATED WORK

We now survey how our work relates to shielding and formal methods, cloud robotics, and networked control systems.

Cloud Robotics: Cloud robotics [14, 18, 19] studies how resource-constrained robots can offload real-time inference [24, 10], distributed learning [9], mapping [21] and control to powerful remote servers. Recent work mitigates network latency by having the cloud only send waypoints or behavioral motion primitives to the robot, which are followed locally using an onboard controller [25]. This work is complementary to ours, since our remote controller can, without loss of generality, send motion primitives, such as options or behavior sub-routines as actions in an MDP. However, our key novelty is to provide a formal *safety* analysis for teleoperation.

Delayed MDPs: A plethora of work in the networked control systems (NCS) community has modeled MDPs with both deterministic and random sensing and actuation delays [2, 17]. However, in stark contrast to our work, these works do not discuss how to formally verify the safety of a shielded controller for those MDPs, especially with logical safety specifications. Moreover, these works do not address how to create a conservative, but realistic, model of stochastic WiFi latency that is a hallmark of our experiments.

$$\Pr(s \models \Box \neg S_{\text{unsafe}}) \geq \delta ; S_{\text{unsafe}} = \{d : d < d_{\text{safe}}\}$$

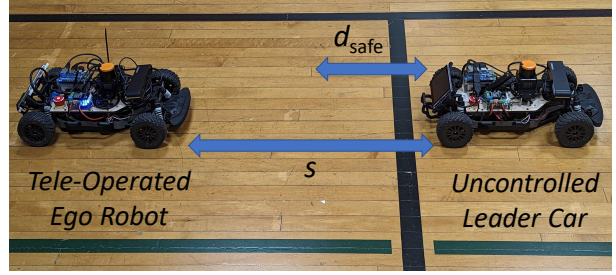


Fig. 2: **Running example/Hardware Setup:** Our teleoperated ego robot (back) must follow a leader car with an unknown trajectory and acceleration profile. The task is to minimize time to a goal while always maintaining a safe distance of more than d_{safe} , as shown in the LTL specification above.

Shielding and Formal Methods: Our work relies on recent advances in reactive synthesis and shielding for safe RL. Given a formal safety specification in linear temporal logic (LTL) and an MDP abstracting the interaction between a robot and its environment, [3] describes how to synthesize a shield. A shield is a filtered list of safe actions that can be enacted in a given MDP state. Importantly, the shield is minimally intrusive, meaning it only disallows an action if it leads to a safety violation. Moreover, the shield only needs to be synthesized once (before learning or real-time execution) using the formal safety specification and the abstracted MDP. For an RL agent that is learning, the shield leads to faster convergence since the agent is stopped from exploring unsafe actions that lead to extremely poor rewards [3]. If the shield is introduced after learning, the agent is more conservative but mitigates the deleterious effects of poor actions. Our work directly uses such advances. However, our key novelty is that we formulate shielding for networked robotics and, to our best knowledge, are the first to demonstrate such a shield on a real robot. Perhaps, the closest work to ours is [16]. Similar to [16], we also focus on shield construction from minimum reachability analysis. However, our approach to shield construction is different and we explain the correlation between our design choices and our system’s performance with the shield.

Reachability Analysis: Another approach to robotic safety is reachability analysis, which uses continuous time dynamic programming to solve the Hamilton Jacobi Isaacs (HJI) equation [5]. For example, we can specify that a robot should reach a goal within a time bound while always avoiding obstacles. However, these methods are hard to scale to high-dimensions and do not allow us to express rich safety specifications, such as “always keep a minimum distance between two vehicles when the network latency is above a threshold and visit landmark A before reaching the goal”, which is possible using the LTL specifications in this paper.

III. BACKGROUND

We describe the required background for our safe networked control approach using the running example in Fig. 2. We focus on discrete-time systems with finite state and action

spaces. For more general control systems, we can often construct a discrete abstraction [4] to apply our approach.

Running example: Consider a resource-constrained mobile robot that must safely follow a leader car or human, which has uncontrolled, stochastic behavior. The sensor observation is transferred to a remote server over a congested wireless link with stochastic network delays. The remote server processes the delayed observation and generates the corresponding control command, which is then transferred back to the controlled mobile robot and executed. The generated control commands must be cognizant of the network delay so that required safety specifications like “do not collide” can be satisfied.

Henceforth, we will use the term *agent* to indicate any controlled entity and *environment* for the rest. The agent and the environment together form the *system*.

A. Linear Temporal Logic (LTL) preliminaries

To address safety, one needs to verify if infinite sequences of system states satisfy certain constraints. The constraints are formally specified using LTL formulae which allow temporal operators like next \bigcirc , until \cup , always \square , and eventually \diamond , in addition to logical operators [4]. LTL has been successfully applied in several robotic motion planning studies.

Let Π be a finite set of atomic propositions that are used to completely describe all system states with respect to the guarantees that we wish to establish. In our running example, we can define an atomic proposition $\pi \in \Pi$ to be True if the distance between the vehicles is less than a safety distance d_{safe} . $\Sigma = 2^\Pi$ denotes the set (of state labels) over which infinite sequences are defined. Then, the set of all possible infinite sequences are represented by Σ^∞ . The LTL formulae follow a specific syntax given by a context-free grammar,

$$\varphi ::= \text{True} \mid \pi \mid \neg\varphi \mid \varphi_1 \wedge \varphi_2 \mid \bigcirc\varphi \mid \varphi_1 \cup \varphi_2, \quad (1)$$

where π is an atomic proposition. Other operators can be obtained from a combination of the above.

We define the satisfaction for an LTL formula φ by an infinite sequence $\sigma = \sigma_0\sigma_1\dots$, $\sigma \in \Sigma^\infty$, i.e., $\sigma \models \varphi$ as,

- 1) $\sigma \models \text{True}$
- 2) $\sigma \models \pi$ iff $\pi \in \sigma_0$ for $\pi \in \Pi$
- 3) $\sigma \models \neg\varphi$ iff $\sigma \not\models \varphi$
- 4) $\sigma \models \varphi_1 \wedge \varphi_2$ iff $\sigma \models \varphi_1$ and $\sigma \models \varphi_2$
- 5) $\sigma \models \bigcirc\varphi$ if $\sigma_1 \models \varphi$
- 6) $\sigma \models \varphi_1 \cup \varphi_2$ iff $\exists j \geq 0$ such that $\sigma_j \models \varphi_1$ and $\sigma_i \models \varphi_2 \forall 0 \leq i < j$.

This allows an LTL formula φ to be represented by a set of infinite sequences that satisfy φ . This set of infinite sequences is called the language of the LTL formula, $\mathcal{W}(\varphi) \in \Sigma^\infty$. In our running example, an LTL formula $\square\neg \text{collide}$ that represents the condition “collision should never happen”, is satisfied by an infinite sequence of system states, each of which has the distance between vehicles to be greater than d_{safe} .

B. Markov Decision Processes

A key contribution of our paper is to develop a formal framework for safe networked robotics. We first define how the agent interacts with the environment in the presence of stochastic latency using a Markov Decision Process (MDP). Then, we verify whether the robot’s decision-making in an MDP satisfies formal safety specifications in LTL.

A *labeled Discrete Time Markov Chain* (DTMC) is a tuple $\langle S, \text{Init}, \mathbb{P}, \Pi, L \rangle$, where S is a finite state set, $\text{Init} \subseteq S$ is the set of initial states, and the transition probability function $\mathbb{P} : S \times S \rightarrow [0, 1]$ satisfies $\sum_{s' \in S} \mathbb{P}(s, s') = 1$. The labeling function $L : S \rightarrow 2^\Pi$ assigns atomic propositions in set Π to each state.

A *labeled Markov Decision Process* (MDP) is a tuple $\langle S, \text{Init}, \text{Act}, \mathbb{P}, \Pi, L \rangle$, where S, Init , and L are the same as in the labeled Markov Chain. The key difference is the introduction of decision-making through the finite set of actions Act , which modifies the transition probability function to $\sum_{s' \in S} \mathbb{P}(s, a, s') = 1$, where $a \in \text{Act}$.

C. LTL formula satisfaction on MDPs

Given an MDP and a candidate control policy, we induce a DTMC that represents system trajectories. We then check if this DTMC satisfies a safety specification.

A path or an infinite sequence of states $s_0s_1\dots$ through a labeled DTMC \mathcal{D} , satisfies the LTL formula φ if $L(s_0)L(s_1)\dots \in \mathcal{W}(\varphi)$. Given a state s , we define the probability of φ to hold at s as $\Pr(s \models \varphi) = \Pr_{\mathcal{D}} \{ \varsigma \in \text{Paths}(s) \mid \varsigma \models \varphi \}$, i.e., the mass of all the paths from s through \mathcal{D} that satisfy the LTL formula φ .

To define satisfaction on MDPs, we first need to resolve the non-determinism in each state (due to the choice of actions) using a scheduler. A memoryless scheduler \mathcal{C} is defined as a mapping from state to actions, $\mathcal{C} : S \rightarrow \text{Act}$. Given the scheduler \mathcal{C} for the MDP \mathcal{M} , the probability of φ holding at s is given by $\Pr(s \models \varphi) = \Pr_{\mathcal{M}^{\mathcal{C}}} \{ \varsigma \in \text{Paths}(s) \mid \varsigma \models \varphi \}$.

D. Safety Specifications

In this work, we focus on safety specifications, which are informally interpreted as “something bad should never happen”. For example, in our robot following scenario, the LTL formula $\square\neg(d < d_{\text{safe}})$ expresses that the distance d between robots should never fall below a safety threshold d_{safe} .

The paths that violate a safety property φ have finite bad prefixes ending in unsafe states. Therefore, satisfying a safety specification $\square\neg S_{\text{unsafe}}$ can be seen equivalently as violating the reachability specification $\diamond S_{\text{unsafe}}$, i.e., $s \models \square\neg S_{\text{unsafe}}$ is equivalent to $s \not\models \diamond S_{\text{unsafe}}$. In simple terms, satisfying “always not unsafe” is equivalent to *violating* “eventually unsafe”. In terms of probability, for a state s , $\Pr(s \models \square\neg S_{\text{unsafe}}) \geq \delta$ is equivalent to $\Pr(s \models \diamond S_{\text{unsafe}}) \leq 1 - \delta$. We request the readers to check [4] for further explanation.

E. Reachability analysis for MDPs

Our goal is to find the optimal set of actions for each system state that minimize the probability of eventually reaching an

unsafe state, which we now define. Given a labeled MDP \mathcal{M} , the scheduler \mathcal{C} , and the set of unsafe states $S_{\text{unsafe}} \subseteq S$ $\Pr_{\mathcal{M}}^{\mathcal{C}}(s \models \diamond S_{\text{unsafe}})$ quantifies a measure of safety for the state $s \in S$. Moreover, the minimum probability of eventually reaching a state in S_{unsafe} from s is given by

$$\Pr^{\min}(s \models \diamond S_{\text{unsafe}}) = \min_{\mathcal{C}} \Pr_{\mathcal{M}}^{\mathcal{C}}(s \models \diamond S_{\text{unsafe}}), \quad (2)$$

where we search over all possible memoryless schedulers. The scheduler $\mathcal{C} = \operatorname{argmin}_{\mathcal{C}} \Pr_{\mathcal{M}}^{\mathcal{C}}(s \models \diamond S_{\text{unsafe}})$ is called the optimal safe scheduler for the given reachability specification. \mathcal{C} achieves the minimum reachability probability or maximum safety probability for state s .

F. Computing minimum reachability probabilities

Our next logical step is to devise an algorithm to find the minimum probability of eventually reaching an unsafe state. Let the vector $(V_s)_{s \in S}$ represent the minimum probability of satisfying the reachability specification $\diamond S_{\text{unsafe}}$ for the MDP \mathcal{M} , i.e., $V_s = \Pr^{\min}(s \models \diamond S_{\text{unsafe}})$. [4] shows that V_s is the unique solution of the following system of linear equations:

$$\begin{aligned} s \in S_{\text{unsafe}} &\Rightarrow V_s = 1 \\ \Pr^{\min}(s \models \diamond S_{\text{unsafe}}) = 0 &\Rightarrow V_s = 0 \\ \Pr^{\min}(s \models \diamond S_{\text{unsafe}}) > 0 \text{ and } s \notin S_{\text{unsafe}} &\Rightarrow \\ V_s = \min \left\{ \sum_{s' \in S} \Pr(s, a, s') V_{s'} \mid a \in \text{Act}(s) \right\} & \end{aligned} \quad (3)$$

Value iteration with the above update rules converges to $V_s = \Pr^{\min}(s \models \diamond S_{\text{unsafe}})$ [4]. First, we assign a value $V_s = 1$ for being an unsafe state (line 1). Then, any state that has zero probability of eventually reaching an unsafe state has a value $V_s = 0$ (line 2). Finally, if the state has a non-zero probability of eventually reaching an unsafe state but is not unsafe itself, we update the value by dynamic programming (line 3). Specifically, we recursively update the value for a state based on the MDP dynamics and the the minimum reachability probability from successor states s' onwards.

However, since our focus is on constructing a shield, we want to find the safest possible action to take in any state. Thus, we are interested in $\Pr^{\min}(\langle s, a \rangle \models \diamond S_{\text{unsafe}})$, which quantifies how safe a specific action a is in the state s if the agent acts according to the optimal safe scheduler from the next time instance onwards. Analogous to the Q-Value in Reinforcement Learning, we call this the state-action value function, or Q-function, $Q_{\langle s, a \rangle}$. Note that $Q_{\langle s, a \rangle}$ can be obtained from V_s as:

$$Q_{\langle s, a \rangle} = \sum_{s' \in S} \mathbb{P}(s, a, s') V_{s'}. \quad (4)$$

The next section describes how the minimum reachability probability (value function) is used to synthesize a shield.

IV. PROBLEM FORMULATION

We assume that the interaction between the agent and the environment *without* network communication can be modeled

as an MDP. MDPs can model a variety of robotic tasks, ranging from manipulation to navigation. Moreover, we can model systems that depend on past history by including sufficient past observations in the state to have a Markovian transition model. In our setup, the agent is controlled remotely, hence a stochastic time delay is introduced into the system. To address this network latency, we first equate our networked control setup to an *MDP with delay*, in particular, observation delay [17]. Such a system has associated with it an observation delay o . This implies that at time t , the recently observed system state is $s_{t-o} \in S$, and any controller for this system can depend only on s_{t-o} . We extend the same argument for network latency, i.e., if τ is the network latency, a control command generated by a remote server/teleoperator corresponding to the delayed state $s_{t-\tau}$ is executed by the agent at time t . Delay τ is the cumulative delay for sending an observation, determining a control, and sending it back to the robot. Now, we consider two approaches for viewing our networked control problem as an MDP with delay:

- 1) A conservative approach is to model our system as an MDP with constant delay τ_{max} , where τ_{max} is the worst-case network latency. For example, this worst-case latency can be obtained from a specific network standard, such as 5G.
- 2) A more sophisticated approach is to consider network latency as part of the environment. Given a latency transition model \mathbb{P}_{τ} , i.e., the transition probabilities of how the latency changes over time, we can model networked control as an MDP with random delays. Crucially, by harnessing the knowledge of the latency transition model, we can stay safe yet make more efficient actions compared to the worst-case approach.

Inspired by [17], we show how to transform MDPs with constant and random delays into equivalent MDPs without delays in Secs. V-A and V-B. Henceforth, we denote these equivalent MDPs as the Networked MDP for constant delay \mathcal{M}_{cd} and random delay \mathcal{M}_{rd} respectively.

For a labeled MDP $\mathcal{M} = \langle S, \text{Init}, \text{Act}, \mathbb{P}, \Pi, L \rangle$, let $S_{\text{unsafe}} \subseteq S$ be the set of bad/unsafe states that the system needs to avoid. A shield can be viewed as a mapping from states to set of actions, designed to enforce a safety specification, such as $\square \neg S_{\text{unsafe}}$. As explained next in Sec. I, we are interested in satisfying safety specifications with a high probability due to the probabilistic nature of environment transitions. We define a δ -shield $C_{\delta} : S \rightarrow 2^{\text{Act}}$ that can enforce this, where δ determines the degree of safety.

Problem Statement: Given a labeled MDP \mathcal{M} that models the interaction between the agent and the environment (basic MDP *without* delay), a latency transition model \mathbb{P}_{τ} , and an upper bound on maximum latency τ_{max} , construct the Networked MDP for constant and random delay, \mathcal{M}_{cd} and \mathcal{M}_{rd} respectively. Further, given the safety specification $\square \neg S_{\text{unsafe}}$, construct a δ -shield for the Networked MDPs.

V. APPROACH

Our key insight is that for systems with network latency, we have access to the prior/delayed system state and the sequence

of actions executed during the delay period. We augment this information into our networked system state and enumerate possible state transitions to develop the Networked MDP.

A. Networked MDP for constant delays

In the constant delay case, we assume that for any time instance t , the latest state available for decision-making is always $s_{t-\tau_{\max}}$. This is a conservative approach since we do not exploit more recent state information for decision-making when network latency drops below τ_{\max} . Since we precisely know the sequence of actions that has been executed by the agent from $t - \tau_{\max}$ to $t - 1$, the maximum information available at time t is $x_t = (s_{t-\tau_{\max}}, a_{t-\tau_{\max}}, a_{t-\tau_{\max}+1}, \dots, a_{t-1})$. Hence, we define x_t to be the networked system state at t . The state space is expanded to be $X_{\text{cd}} = S \times \text{Act}^{\tau_{\max}}$ but the action space remains the same. We define the initial states set as $\text{Init} \times (a_s, a_s, \dots, a_s)$, where a_s refers to the action that does not alter the robot state.

The transition probability function $\mathbb{P}_{\text{cd}} : X_{\text{cd}} \times \text{Act} \times X_{\text{cd}} \rightarrow [0, 1]$ is defined as follows. Let the state be $x = (s, a_0, \dots, a_{\tau_{\max}-1}) \in X_{\text{cd}}$, then

$$\mathbb{P}_{\text{cd}}(x, a, x') = \begin{cases} \mathbb{P}(s_0, a_0, s') & \text{if } x' = (s', a_1, \dots, a) \\ 0 & \text{otherwise,} \end{cases} \quad (5)$$

where a is the action proposed to be executed on x . We define the labeling function $L_{\text{cd}} : X_{\text{cd}} \rightarrow 2^\Pi$ as $L_{\text{cd}}(x) = L(s)$. Intuitively this makes sense because a path through the networked MDP will still contain all the system states but with a constant delay. Hence, if a path through the original MDP \mathcal{M} is safe/unsafe, the corresponding path through the networked MDP should also be safe/unsafe respectively. The labeled networked MDP \mathcal{M}_{cd} for constant delay is the tuple $\langle X_{\text{cd}}, \text{Init}_{\text{cd}}, \text{Act}, \mathbb{P}_{\text{cd}}, \Pi, L_{\text{cd}} \rangle$, where the constant delay is the maximum network latency τ_{\max} .

B. Networked MDP for random delays

Unlike the constant delay case, here we utilize the latest available state observation $s_{t-\tau_t}$ for decision-making, where $\tau_t \in [0, \tau_{\max}]$ is the current delay value. We define the delay at t to be a random variable $\Omega_t \in \{0, 1, \dots, \tau_{\max}\}$, where τ_{\max} is the maximum network latency. We assume a probabilistic transition model that governs the delay transitions. Specifically, we model the delay transition as a conditional probability distribution $\mathbb{P}(\Omega_{t+1} = \tau' | \Omega_t = \tau) = \mathbb{P}_\tau(\tau, \tau')$ which has the following properties:

- 1) $\mathbb{P}_\tau(\tau_{\max}, \tau') = 0$ if $\tau' > \tau_{\max}$. This ensures that the delay cannot increase beyond τ_{\max} .
- 2) $\mathbb{P}_\tau(\tau, \tau') = 0$ if $\tau' > \tau + 1$. This implies that the delay cannot increase by more than one time step in a single transition. This property is naturally enforced in practice. For the current time step, if no new control command is received from the remote server/teleoperator, we continue to work with the previously executed action. Thus the delay increases by 1. On the other hand, if we receive a new control command, then it implies that the delay is the same or has reduced.

Analogous to the constant delay case, at time t , we have access to the sequence of actions that the agent has executed from $t - \tau_t$ to $t - 1$. Since τ_t is upper-bounded by τ_{\max} , the maximum length of the sequence of actions available at t is τ_{\max} . The state x_t is defined to be $(s_{t-\tau_t}, a_{t-\tau_t}, \dots, a_{t-1}, \phi, \dots, \phi, \tau_t)$, i.e., x_t contains τ_t number of valid actions and $\tau_{\max} - \tau_t$ number of invalid or empty actions indicated by ϕ . We introduce ϕ to ensure the state size remains constant. Note that the state also includes the current delay value. The state space is thus $X_{\text{rd}} = S \times (\text{Act} \cup \{\phi\})^{\tau_{\max}} \times \Omega$. Without loss of generality, we assume that the initial delay is 0, as the control command corresponding to the initial system state will be available to the agent. The initial states set is then $\text{Init} \times (\phi, \phi, \dots, \phi) \times \{0\}$.

We now define the transition probability function $\mathbb{P}_{\text{rd}} : X_{\text{rd}} \times \text{Act} \times X_{\text{rd}} \rightarrow [0, 1]$.

$$\mathbb{P}_{\text{rd}}(x_t, a_t, x_{t+1}) = \begin{cases} \mathbb{P}_\tau(\tau_t, \tau_{t+1}), & \text{if } \tau_{t+1} = \tau_t + 1 \\ & x_{t+1} = (s_{t-\tau_t}, a_{t-\tau_t}, \dots, a_t, \phi, \dots, \phi, \tau_t + 1) \\ \mathbb{P}_\tau(\tau_t, \tau_{t+1}) y_{t-\tau_t} \underbrace{\sum_{s_{t-\tau_t+1} \in S} y_{t-\tau_t+1} \dots \sum_{s_t \in S} y_t}_{\tau_t+1 \text{ times}}, & \text{if } \tau_{t+1} = 0 \\ & x_{t+1} = (s_{t+1}, \phi, \dots, \phi, 0) \\ \mathbb{P}_\tau(\tau_t, \tau_{t+1}) y_{t-\tau_t} \underbrace{\sum_{s_{t-\tau_t+1} \in S} y_{t-\tau_t+1} \dots \sum_{s_{t-\tau_{t+1}} \in S} y_{t-\tau_{t+1}}}_{\tau_t-\tau_{t+1}+1 \text{ times}}, & \text{if } 0 < \tau_{t+1} \leq \tau_t \\ & x_{t+1} = (s_{t+1-\tau_{t+1}}, a_{t+1-\tau_{t+1}}, \dots, a_t, \phi, \dots, \phi, \tau_{t+1}) \\ 0 & \text{otherwise,} \end{cases} \quad (6)$$

where $y_{t-\tau_t} = \mathbb{P}(s_{t-\tau_t}, a_{t-\tau_t}, s_{t-\tau_t+1})$. For an action a_t , if the networked system transitions from state x_t with delay τ_t to state x_{t+1} with delay τ_{t+1} , the first $\tau_t - \tau_{t+1} + 1$ valid actions in x_t need to be executed so that the number of valid actions in x_{t+1} after appending a_t is τ_{t+1} . This leads to the $\tau_t - \tau_{t+1} + 1$ products in Eq. 6.

To gain better intuition, we look at examples of transitions. Given a state $x_t = (s_{t-\tau_t}, a_{t-\tau_t}, \dots, a_{t-1}, \phi, \dots, \phi, \tau_t)$ and action a_t , we divide the possible transitions into the following three cases:

- *Case 1:* If no new control command is received from the remote server/teleoperator, the delay corresponding to $t + 1$ should be $\tau_t + 1$. The latest available state observation does not change, and the state x_{t+1} is given by $(s_{t-\tau_t}, a_{t-\tau_t}, \dots, a_t, \phi, \dots, \phi, \tau_t + 1)$. Notice that a_t gets appended to the sequence of actions. This is consistent with our definition of the state as the number of valid actions is $\tau_t + 1$, which is the delay of the latest available state

observation.

- *Case 2:* If the control command corresponding to the current system state s_{t+1} is received, there is no delay i.e., τ_{t+1} is 0. Thus, the state x_{t+1} is given by $(s_{t+1}, \phi, \dots, \phi, 0)$. Again, this is consistent with our definition of the state as the number of valid actions is 0 which is the delay of the latest available state observation.
- *Case 3:* If the control command corresponding to the system state with delay τ' , namely $s_{t+1-\tau'}$, is received, then τ_{t+1} is τ' . The state x_{t+1} is given by $(s_{t+1-\tau'}, a_{t+1-\tau'}, \dots, a_t, \phi, \dots, \phi, \tau')$.

Similar to the constant delay case, the labeling function is $L_{rd} : X_{rd} \rightarrow 2^{\Pi}$ as $L_{rd}(x_t) = L(s_{t-\tau_t})$, where τ_t is the delay at t . Thus, the labeled networked MDP \mathcal{M}_{rd} for random delay is the tuple $\langle X_{rd}, \text{Init}_{rd}, \text{Act}, \mathbb{P}_{rd}, \Pi, L_{rd} \rangle$.

C. Shield Construction and Safe Networked Control

Having shown how to obtain the Networked MDPs, we now describe the process of constructing a δ -shield for the same. For any MDP and a set of unsafe states $S_{\text{unsafe}} \subseteq S$, we want the system to satisfy the safety specification $\square \neg S_{\text{unsafe}}$ with high probability. As explained in Sec. III-D, we can reformulate this problem as satisfying the reachability specification $\diamond S_{\text{unsafe}}$ with low probability. Therefore, we construct the shield so that the probability of satisfying $\diamond S_{\text{unsafe}}$ is minimized. First we calculate $Q_{\langle s,a \rangle}$ for all $\langle s,a \rangle \in S \times \text{Act}$ as described in Sec. III-F. With the $Q_{\langle s,a \rangle}$ values, we define the shield as follows.

Definition: A δ -shield $C_\delta : S \rightarrow 2^{\text{Act}}$, for any state $s \in S$, and $\delta \in [0, 1]$ is

$$C_\delta(s) = \begin{cases} a \mid a \in \text{Act}(s) \ \& \ Q_{\langle s,a \rangle} \leq 1 - \delta & \text{if } V_s \leq 1 - \delta \\ \operatorname{argmin}_a Q_{\langle s,a \rangle} & \text{if } V_s > 1 - \delta. \end{cases} \quad (7)$$

Intuitively, for a state s with $V_s \leq 1 - \delta$, $C_\delta(s)$ is the set of actions, following which if the agent acts optimally (see Sec. III-F), $\Pr(s \models \diamond S_{\text{unsafe}}) \leq 1 - \delta$. Thus if the control command from the remote server/teleoperator belongs to $C_\delta(s)$, then the control command is executed. Else, the control command is overwritten with the action $a \in C_\delta(s)$ that offers the highest task efficiency.

However, due to stochastic environment transitions dictated by the probabilistic transition function \mathbb{P} , even if $a \in C_\delta(s)$ is executed, the system can transition to a state with $V_s > 1 - \delta$. In such cases, the shield overwrites the control command from the remote server/teleoperator such that the agent executes the optimal safe scheduler.

It is important to note that an action a for the system state s can guarantee $Q_{\langle s,a \rangle}$ as the probability of reaching S_{unsafe} only if the optimal safe scheduler is executed following a . However, this does not happen as we invoke the shield at every system state. So, we cannot guarantee $\Pr(s \models \diamond S_{\text{unsafe}}) \leq 1 - \delta$ in expectation, which is already noted in [16].

δ is a design parameter that dictates the safety-efficiency trade-off of our networked control system as we will see in Sec. VI. A δ -shield for the MDP is constructed by applying

δ -shields to all states. The shield is *minimally intrusive* in the sense that for a system state s , given the control command a received from the remote server/teleoperator, it is overwritten by the shield only if $Q_{\langle s,a \rangle} \leq 1 - \delta$.

Special case, $\delta = 1.0$: Setting $\delta = 1.0$ ensures absolute safety. If a state $s \in S$ has $V_s = 0$, there exists an action $a \in \text{Act}(s)$ such that $Q_{\langle s,a \rangle} = 0$. This implies for all $s' \in S$ such that $\mathbb{P}(s, a, s') > 0$, we have $V_{s'} = 0$. Thus, starting from a state s for which $V_s = 0$, and executing an action a such that $Q_{\langle s,a \rangle} = 0$, allows us to stay in states for which V_s is always 0. This implies that the system state $s \notin S_{\text{unsafe}}$, and the system forever remains in the set of safe states. The similarity of our approach to the shield synthesis approach in [3] is described in the Appendix.

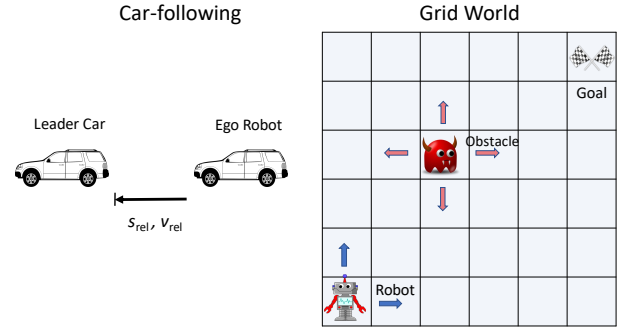


Fig. 3: **Simulations:** (Left) The state in the car-following scenario is the relative distance and velocity. (Right) The robot must reach the goal while avoiding the red obstacle.

VI. SIMULATION EXPERIMENTS

Our simulations highlight how our shielding approach enables a robot to flexibly behave more conservatively during larger delays, but also more aggressively with lower delays. Intuitively, we expect to observe this behavior as the uncertainty in environment evolution increases with increasing delay.

A. Environments and Safety Specification

Grid World: We consider a grid world environment with a controlled robot/agent and a dynamic obstacle/adversary illustrated in Fig. 3. Given an $n \times n$ grid, the agent is initially positioned at the bottom left and is tasked with reaching the goal at the top right of the grid. The obstacle has a uniform probability of moving one step in any direction. The robot can be controlled to move one step in any direction or stay on the same grid. At any time-step t , the robot state is given by its position on the grid, $r_t = (r_{x_t}, r_{y_t})$. The obstacle state is similarly $o_t = (o_{x_t}, o_{y_t})$ and the system state is defined to be $s_t = (r_t, o_t)$. In our experiments, we set $n = 8$, initialize the obstacle randomly, and simulate finite-horizon episodes of length 50 time steps. An episode is considered a *win* if the robot reaches the goal without colliding, a *loss* if there is a collision, or a *draw* otherwise. We use tabular Q-learning to design an off-the-shelf controller for the basic MDP without network latency. The controller is designed to satisfy the robot's objective to maximize wins. Our aim is to construct a shield, to ensure safety in the presence of stochastic latency,

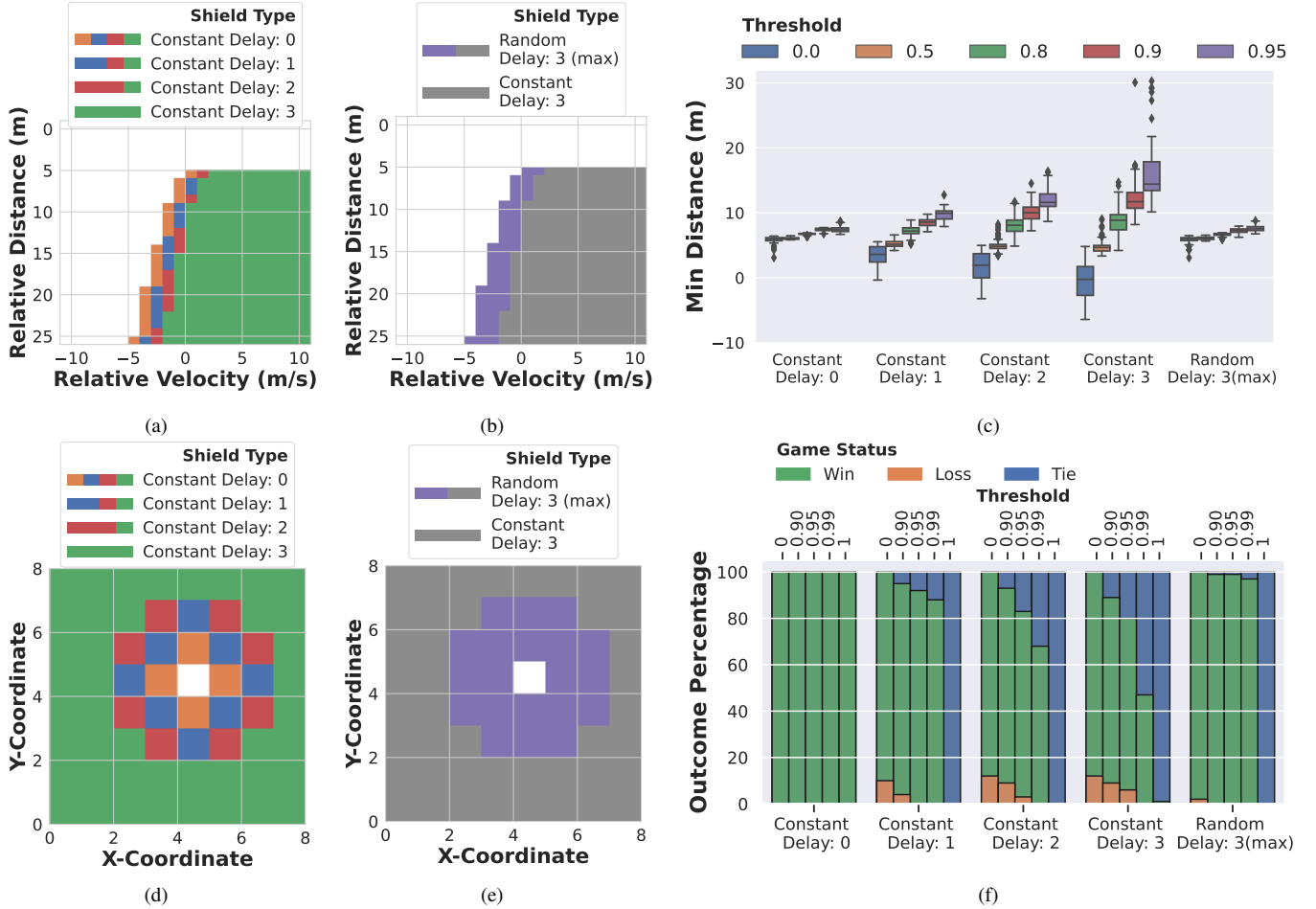


Fig. 4: **Shielding leads to safe networked control in simulations.** Top row - Car following simulation results; Bottom row - Grid world simulation results. Figs. 4a and 4d show that the set of safe initial states ($\delta = 0.95$) for the Networked MDP for a range of constant maximum delays increases as the latency decreases. This is depicted by the legend that has multiple colors attributed to lower latencies, where tighter closed-loop control is possible. For smaller delays, we are allowed to have a smaller initial relative distance and relative velocity for car following, and a smaller initial distance between the robot and the obstacle for the grid world. We refer to this as *aggressive initialization*. Figs. 4b and 4c show the set of safe initial states ($\delta = 0.95$) for random delay (maximum delay of 3 time steps) and constant delay (3 time steps). We observe that aggressive initialization is possible for the random delay case and not for the constant delay case, since the former exploits the knowledge of the latency transition model to act more nimbly. Figs. 4c and 4f show that as latency increases, the system tends to be conservative, leading to increased distances in the car-following scenario, and increased number of ties in the grid world case.

for the specification $\neg S_{\text{unsafe}} \cup \text{goal}_t$, where S_{unsafe} is the set of states that satisfy the atomic propositions, $(r_x = o_x)$ and $(r_y = o_y)$. Here, (r_x, r_y) represents the robot location, and (o_x, o_y) represents the obstacle’s location in the grid.

Car-following: In this environment, the setup is similar to our running example explained in Sec. III. The controlled ego robot has to follow the uncontrolled leader car, see Figs. 3 and 2. We first discretize the system by constructing a finite state-action abstraction of the same. Now, the state at time t is defined to be $(s_{\text{rel},t}, v_{\text{rel},t})$, where $s_{\text{rel},t}$ is the distance between the two vehicles, and $v_{\text{rel},t}$ is the relative velocity. Similar to the grid world, we consider finite-horizon interactions between the ego-robot and the leader car, with episode lengths of 100 time steps. For the off-the-shelf controller, we train a Deep RL agent to maximize distance travelled and minimize collision. For the specification $\square \neg S_{\text{unsafe}}$, we aim to construct a shield

that ensures safety in the presence of stochastic latency. S_{unsafe} indicates the set of states that satisfy the atomic proposition $(s_{\text{rel}} < d_{\text{safe}})$ meters.

Further details on training the RL agent, including the benefits of shielding *during* learning, can be found in the Appendix.

B. Results

First, we obtain key intuition about our safe networked control approach by observing the set of safe initial states in our networked MDP for constant delay. By safe initial states, we refer to the initial states (as defined in Sec. V-A) with $V_s \leq 1 - \delta$. Figs. 4a and 4d show that the set of safe initial states decreases for larger delays. In the grid world environment, the robot has to stay far away from the obstacle initially for larger delays. Similarly for the car-following scenario, the ego robot has to maintain a larger relative distance and relative

velocity from the leader car initially. However, as the latency decreases, the set of safe states expands, allowing the robot to act more nimbly within a closer distance to other agents.

We now explain how our safe networked control approach ensures a safety-efficiency trade-off with varying latency. By safety-efficiency trade-off, we mean the robot acts more safely if the delay is larger, but flexibly acts more aggressively if the delay decreases. Additionally, we analyze how the choice of δ affects such a trade-off.

How does the performance of our safe networked control approach vary with latency?: We analyze the task performance for the constant delay case. For a fixed δ , with increasing maximum latency, the networked system performs less efficiently, prioritizing safety. In the grid world, the number of wins decreases and the number of ties increases (see Fig. 4f). Essentially, with larger delays, the robot cannot aggressively move towards the top right due to uncertainty over the obstacle’s position, and must act cautiously to avoid the obstacle at all costs. As such, it effectively sacrifices its goal for a tie. Similarly, in the car-following scenario, the minimum distance maintained from the leader robot increases (Fig. 4c). Intuitively, the robot might take longer to reach its destination by virtue of keeping a larger safety margin.

How does δ affect the safety-efficiency trade-off?: We look at the task performance for the constant delay case for a fixed maximum latency and increasing δ . Recall that $\delta = 1$ corresponds to absolute safety and higher values of δ lead to more conservative behavior with more restrictions from the shield. As such, we see that the task efficiency decreases as safety is increasingly prioritized with higher δ . In the grid world, Fig. 4f shows a lesser number of wins and a larger number of ties. Similarly, for car-following, the aggregate minimum distance maintained from the leader robot increases (Fig. 4c). Importantly, $\delta = 0$ is a purely un-shielded approach, which leads to collisions (losses) or violation of the safety margin.

How does the modeling choice i.e., Networked MDP for constant delay vs. random delay, affect safety and efficiency?: We now illustrate that, by incorporating the latency transition model \mathbb{P}_τ , a shield synthesized for a random delay performs more efficiently than one for a constant delay since the latter always prepares for the worst case. To do so, we compare the networked MDP for constant delay of τ_{\max} is 3 against the networked MDP for random delay which uses the latency transition model \mathbb{P}_τ . First, Figs. 4b and 4e show that the set of safe initial states is larger for the random delay case in comparison to the constant delay case for both environments. Secondly, for a fixed δ , the task efficiency is higher in the random delay case. This implies more wins and fewer draws in the grid world, and lower aggregate distance maintained during car following as seen in Figs. 4f and 4c respectively. To summarize, we infer that incorporating the latency transition model in our MDP design allows for efficient task performance. However, in both environments, there is no reduction in safety probability. Thus, the improvement in efficiency does not come at the cost of safety.

VII. REAL WORLD DEMONSTRATION

We now demonstrate the running example in Figs. 1 and 2 in a hardware experiment. Both the uncontrolled leader car and our ego-robot use a variant of the standard F1/10th design [22]. Both robots have an Nvidia Jetson TX2 embedded GPU, Orbbec Astra Pro RGB-D camera, and a Hokuyo Laser rangefinder. The ego-robot measures a laser point cloud containing 1080 range values, which it sends over WiFi using ROS to a remote Nvidia desktop GPU (the “cloud”). At the remote GPU, the point cloud is processed, and a time-optimal controller computes the actions, which are sent back over WiFi to the robot. Then, the robot invokes the shield as a pre-computed look-up table that has the list of $Q_{\langle s,a \rangle}$ for all state-action pairs in the networked MDP. This allows us to modify the shield during runtime, if required, by changing δ . The shield is extremely fast since it is a look-up table invoked in C++. Formally, our safety specification is $\Box \neg S_{\text{unsafe}}$, shown in Fig. 2. Our objective is to minimize the time taken for our ego-robot to reach a goal while always maintaining a safe distance between the vehicles. We now demonstrate how to construct our Networked MDP using real WiFi data and show experimental results of our safe networked control approach.

How do we construct a Networked MDP using real WiFi network traces?: Fig. 6 shows an example aggregate of multiple time series of measured WiFi latency. From the observed WiFi latency time series, we set 300 ms as the maximum network latency. We consider latency bins of size 100 ms and construct a latency transition model \mathbb{P}_τ . Such Markov transition models are extensively used in the networking literature [20]. Given \mathbb{P}_τ , we construct our Networked MDP for random delay. We use the worst-case upper bound to construct the Networked MDP for constant delay. Next, we assume bounds on the behavior of the uncontrolled leader car, such as its maximum speed and acceleration/deceleration. These bounds can be flexibly set by a designer based on domain knowledge. Laxer bounds lead to greater uncertainty in environment transitions, resulting in conservative behavior of the ego-robot.

Does a minimally intrusive shield always lead to safety?: Fig. 5a shows a real trajectory of the uncontrolled leader and our ego-robot for the unshielded and shielded cases. The shield overwrites control commands when close to the leader car, and is inactive when further away.

This is clearly observed in the constant delay case. The shield always overwrites the time-optimal controller’s output when the distance between the cars drops below ~ 1.7 meters. On the other hand, the shield never overwrites the controller’s output when the distance between the cars is above ~ 2.25 meters.

How do shields gracefully trade off safety and efficiency?: First, the trend in Fig. 5 validates our simulations in Fig. 4. Namely, the distance between the vehicles increases as the network latency rises since the ego-robot must be more conservative to account for delayed sensory information. This is clearly visible in the trajectory plot with the shield for

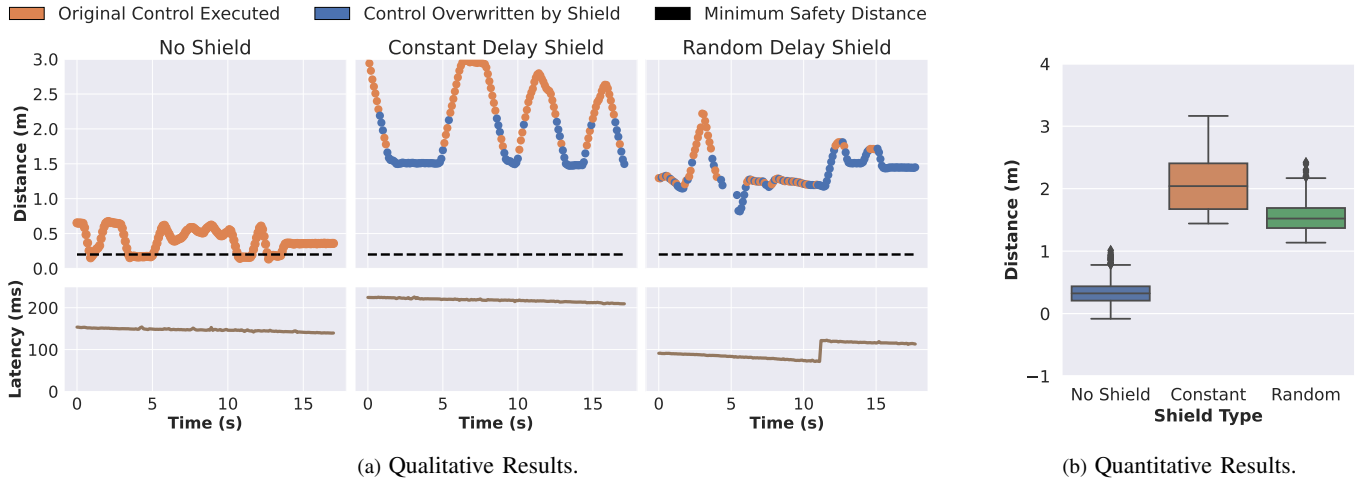


Fig. 5: **Real World Demonstration Results.** Fig. 5a shows recorded trajectories from our real-world leader-follower test bed. We observe that, without our shield, the networked control system fails to satisfy the safety specification of “always remain at least 0.2 meters away”. However, our safe networked control approach is able to satisfy the safety specification, for both constant and random delays. Further, notice that our shield is *minimally intrusive*, i.e., with constant delay, the shield is never invoked when the distance between the two cars is more than ~ 2.25 meters. Also, as seen in Fig. 5b, the shield for the random delay case exploits our knowledge of expected WiFi latency transitions rather than assume the worst case latency, which allows the ego robot to follow the leader car at a closer distance.

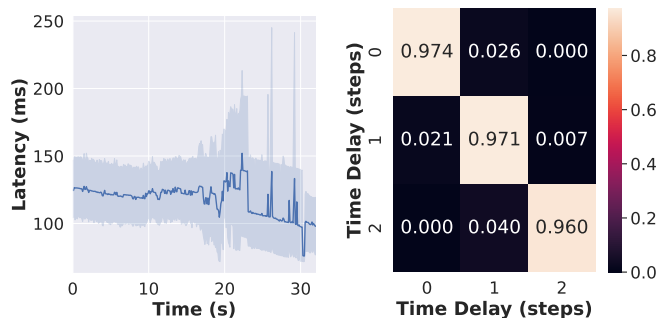


Fig. 6: **Wi-Fi Performance:** (Left) Aggregate Wi-Fi latency time-series showing dynamic changes in latency over time, averaged over multiple runs. (Right) We represent the probability of transitioning between 3 discrete WiFi latency bins as a heatmap, which is used in our Networked MDP for random delay.

random delay (Fig. 5a). During the initial 10s, when the networked system has a delay of less than 100 ms, the average distance maintained is less than 1.25 meters. Then, when the delay is about 200 ms, the ego-robot trades efficiency for safety by maintaining a larger distance of around 1.5 meters.

Second, we clearly see that a constant delay shield must account for the worst-case WiFi latency and thus ensures a higher distance between vehicles, in comparison to a random delay shield. Fig. 5b illustrates this for 10 runs with different conditions. This difference in safety distance is statistically significant with a Wilcoxon p -value < 0.001 .

Further experiments in the Appendix: Our Appendix shows the utility of using a shield for safe reinforcement learning in systems with network delay during the training process. Moreover, we present further hardware experiments with a human tele-operator in the loop and discuss the formal

complexity of shield synthesis.

Limitations: A promising future direction is *shared* autonomy between a robot and human teleoperator or cloud controller. In principle, our method applies if we know an abstraction of the robot’s MDP and when it offloads computation to the cloud. However, our experiments do not yet test shared autonomy.

VIII. CONCLUSION AND FUTURE DIRECTIONS

To our best knowledge, this paper is the first to develop and deploy a rigorous shield for safe teleoperated control over stochastic wireless links. Our key insight is to cast networked control with stochastic latency as an MDP with delayed sensory observations. Our work is timely since we are seeing a surge of teleoperated robots, ranging from remote take-overs of autonomous vehicles to food delivery robots. In future work, we plan to deploy our robot on a 5G network and compare the safety vs. efficiency trade-off compared to WiFi. Second, we will address shared autonomy where the robot has a local control loop that dynamically asks for help from a human.

REFERENCES

- [1] Who's driving that food delivery bot? it might be a gen z gamer. <https://www.latimes.com/business/story/2022-03-17/california-autonomous-sidewalk-food-delivery-robots-coco-starship-kiwibot>, 2022. [Online; accessed 03-Feb.-2022].
- [2] Sachin Adlakha, Sanjay Lall, and Andrea Goldsmith. Networked markov decision processes with delays. *IEEE Transactions on Automatic Control*, 57(4):1013–1018, 2011.
- [3] Mohammed Alshiekh, Roderick Bloem, Rüdiger Ehlers, Bettina Könighofer, Scott Niekum, and Ufuk Topcu. Safe reinforcement learning via shielding. In *Proceedings of the AAAI Conference on Artificial Intelligence*, volume 32, 2018.
- [4] Christel Baier and Joost-Pieter Katoen. *Principles of model checking*. MIT press, 2008.
- [5] Somil Bansal, Mo Chen, Sylvia Herbert, and Claire J Tomlin. Hamilton-jacobi reachability: A brief overview and recent advances. In *2017 IEEE 56th Annual Conference on Decision and Control (CDC)*, pages 2242–2253. IEEE, 2017.
- [6] Francesco Borrelli, Alberto Bemporad, and Manfred Morari. *Predictive control for linear and hybrid systems*. Cambridge University Press, 2017.
- [7] Eduardo F Camacho and Carlos Bordons Alba. *Model predictive control*. Springer Science & Business Media, 2013.
- [8] Karthik Chandrasekaran, Suraj Parameswaran, Srikanth Annamraju, Sourav Chandra, Ramalingam Manickam, and Asokan Thondiyath. A practical approach to the design and development of tele-operated surgical robots for resource constrained environments—a case study. *Journal of Medical Devices*, 15(1), 2021.
- [9] Sandeep Chinchali, E. Pergament, M. Nakanoya, E. Cidon, E. Zhang, D. Bharadia, M. Pavone, and S. Katti. Harvestnet: Mining valuable training data from high-volume robot sensory streams. In *2020 International Symposium on Experimental Robotics (ISER)*, Valetta, Malta, 2020.
- [10] Sandeep Chinchali, Apoorva Sharma, James Harrison, Amine Elhafsi, Daniel Kang, Evgenya Pergament, Eyal Cidon, Sachin Katti, and Marco Pavone. Network offloading policies for cloud robotics: a learning-based approach. *Autonomous Robots*, pages 1–16, 2021.
- [11] Giuseppe De Giacomo and Moshe Y Vardi. Linear temporal logic and linear dynamic logic on finite traces. In *IJCAI'13 Proceedings of the Twenty-Third international joint conference on Artificial Intelligence*, pages 854–860. Association for Computing Machinery, 2013.
- [12] Oussama El Marai, Tarik Taleb, and JaeSeung Song. Ar-based remote command and control service: Self-driving vehicles use case. *IEEE Network*, 2022.
- [13] Issam El Rassi and Jean-Michel El Rassi. A review of haptic feedback in tele-operated robotic surgery. *Journal of medical engineering & technology*, 44(5):247–254, 2020.
- [14] Ken Goldberg and Ben Kehoe. Cloud robotics and automation: A survey of related work. *EECS Department, University of California, Berkeley, Tech. Rep. UCB/EECS-2013-5*, 2013.
- [15] Ankur Handa, Karl Van Wyk, Wei Yang, Jacky Liang, Yu-Wei Chao, Qian Wan, Stan Birchfield, Nathan Ratliff, and Dieter Fox. Dexpivot: Vision-based teleoperation of dexterous robotic hand-arm system. In *2020 IEEE International Conference on Robotics and Automation (ICRA)*, pages 9164–9170. IEEE, 2020.
- [16] Nils Jansen, JSL Junges, and AC Serban. Safe reinforcement learning using probabilistic shields. *Dagstuhl: Schloss Dagstuhl*, 2020.
- [17] Konstantinos V Katsikopoulos and Sascha E Engelbrecht. Markov decision processes with delays and asynchronous cost collection. *IEEE transactions on automatic control*, 48(4):568–574, 2003.
- [18] Ben Kehoe, Sachin Patil, Pieter Abbeel, and Ken Goldberg. A survey of research on cloud robotics and automation. *IEEE Trans. Automation Science and Engineering*, 12(2):398–409, 2015.
- [19] J Kuffner. Cloud-enabled robots in: Ieee-ras international conference on humanoid robots. *Piscataway, NJ: IEEE*, 2010.
- [20] Hongzi Mao, Ravi Netravali, and Mohammad Alizadeh. Neural adaptive video streaming with pensieve. In *Proceedings of the conference of the ACM special interest group on data communication*, pages 197–210, 2017.
- [21] Gajamohan Mohanarajah, Dominique Hunziker, Raffaello D'Andrea, and Markus Waibel. Rapyuta: A cloud robotics platform. *IEEE Transactions on Automation Science and Engineering*, 12(2):481–493, 2015.
- [22] Matthew O'Kelly, Varundev Sukhil, Houssam Abbas, Jack Harkins, Chris Kao, Yash Vardhan Pant, Rahul Mangharam, Dipshil Agarwal, Madhur Behl, Paolo Burgio, et al. F1/10: An open-source autonomous cyber-physical platform. *arXiv preprint arXiv:1901.08567*, 2019.
- [23] Hang Su, Juan Sandoval, Pierre Vieyres, Gérard Poisson, Giancarlo Ferrigno, and Elena De Momi. Safety-enhanced collaborative framework for tele-operated minimally invasive surgery using a 7-dof torque-controlled robot. *International Journal of Control, Automation and Systems*, 16:2915–2923, 2018.
- [24] Ajay Kumar Tanwani, Nitesh Mor, John D. Kubiawicz, Joseph E. Gonzalez, and Ken Goldberg. A fog robotics approach to deep robot learning: Application to object recognition and grasp planning in surface decluttering. *2019 International Conference on Robotics and Automation (ICRA)*, pages 4559–4566, 2019.
- [25] Nan Tian, Ajay Kumar Tanwani, Ken Goldberg, and Somayeh Sojoudi. Mitigating network latency in cloud-based teleoperation using motion segmentation and synthesis. In *Robotics Research: The 19th International*

Symposium ISRR, pages 906–921. Springer, 2022.

- [26] Josiah Wong, Albert Tung, Andrey Kurenkov, Ajay Mandlekar, Li Fei-Fei, Silvio Savarese, and Roberto Martín-Martín. Error-aware imitation learning from teleoperation data for mobile manipulation. In *Conference on Robot Learning*, pages 1367–1378. PMLR, 2022.
- [27] Tianhao Zhang, Zoe McCarthy, Owen Jow, Dennis Lee, Xi Chen, Ken Goldberg, and Pieter Abbeel. Deep imitation learning for complex manipulation tasks from virtual reality teleoperation. In *2018 IEEE International Conference on Robotics and Automation (ICRA)*, pages 5628–5635. IEEE, 2018.

IX. APPENDIX

A. Overview and Table of Contents

Our appendix is divided as follows.

- First, we describe our safe networked control approach with teleoperation in Sec. IX-B. We explain our setup and quantify the teleoperation efficiency by monitoring the distance maintained by the ego robot from the leader car.
- Then, we briefly discuss the complexity associated with our shield construction in Sec:IX-C
- In Sec. IX-D, we describe how to integrate our shield C_δ with the RL paradigm for Safe RL [3]. We also discuss the results of Safe RL implementation for our networked control system.
- Finally, we describe in detail our simulation and real world demonstration environments.

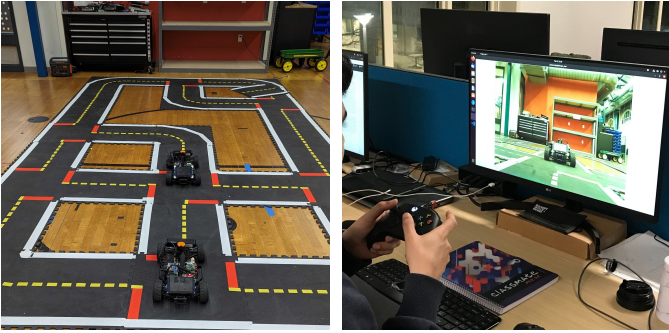


Fig. 7: **Teleoperation Setup.** The camera image on the left depicts the real-world car-following teleoperation setup. The ego robot located behind the leader car is remotely operated by viewing RGB camera images streamed from the robot. The photo on the right shows the user controlling the agent via an Xbox gamepad.

B. Teleoperation with a Human-in-the-Loop

We now show the flexibility of our approach – we can, without loss of generality, shield an automatic controller or the actions of a *human* teleoperator. To do so, we repeat the exact same hardware experiment, but instead take remote commands from a human who controls the robot using an Xbox controller connected over WiFi as shown in Fig. 7.

We run trials with 5 different human operators to accrue a diversity of experimental results. It is observed that the random delay shield protects the ego-robot from collisions even when the teleoperator controls the robot using time-delayed and often jittery video streams. Fig. 8 confirms that the shield creates a statistically significant change in distance and gracefully adapts the safety margin based on the real-time WiFi latency.

This use case is very important, since many teleoperated robots, such as fleets of food delivery robots, are increasingly being controlled from remote command centers. Since outdoor network connectivity is often stochastic, the random delay shield can act as a viable option for addressing the effects of latency on control.

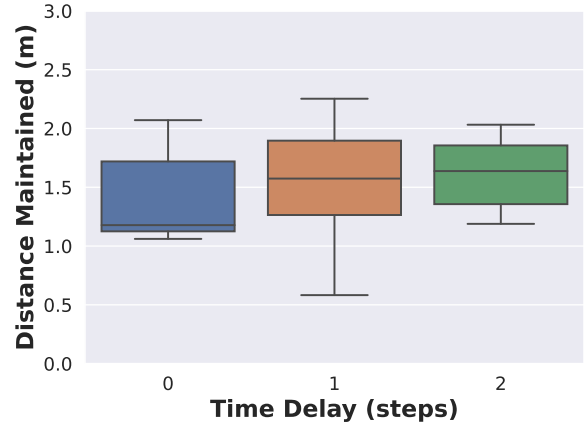


Fig. 8: **Teleoperation with random delay shield.** The figure illustrates the distribution of the distances maintained by the ego robot from the leader vehicle during 5 car-following trials from different teleoperators. The shield ensures that the robot is cognizant of the stochastic network latency and alters its behaviour accordingly. As expected, the robot acts conservatively with increasing network delay.

C. Complexity of Synthesis

We now quantify the computational complexity of synthesizing a shield. We have seen that construction of the shield involves computing minimum reachability probabilities for the MDP given a set of unsafe states. It is known that for finite MDPs, like in our case, this computation can be done in time polynomial in the size of the MDP [4]. Recall that in our Networked MDP, the augmented state contains the latest state observation and a history of the actions thereafter. Thus, the size of the state space has expanded from $|S|$ to $|S||\text{Act}|^{\tau_{max}}$, while the action space size remains the same. The time complexity for constructing the shield for the Networked MDP is then polynomial in its size which is computed using the size of the augmented state space.

D. Benefits of Training using a Shield

We now discuss the benefits of training a data-driven controller, such as an RL agent, with a shield during the learning process. As stated in the related work section of the main paper, [3] illustrates that using a shield during RL training leads to faster convergence since the agent is disallowed from exploring unsafe actions that lead to extremely poor rewards.

We now ask whether the safe benefits occur for an RL agent *with delayed observations* such as in our delayed MDP. The reinforcement learning problem with the shield is set as follows. Let τ_{max} be the maximum latency, then, at any time step, the RL agent has access to the tuple $(s_{t-\tau_{max}}, a_t, s_{t-\tau_{max}+1}, r_{t+1})$. This can be considered as a system with observation delay, and in Sec. V, we have shown how network latency/delay can be equated to observation delay. We use the post-posed shielding approach, and assign the reward at t , r_{t+1} , to the agent’s selected action a_t as shown in [3]. Thus, the shield on the robot-end, substitutes the action suggested by the agent if the action is deemed unsafe with



Fig. 9: **Safe Reinforcement Learning.** The figure shows the learning curves for RL agents that we use as our off-the-shelf controller in both environments. The top row shows the learning phase with and without shield for the car-following scenario. Observe that the unshielded case results in violation of the safety specification. For the shielded case, we implement the shield C_δ as defined in Eq. 7. In our experiments, we set $\delta = 0.95$. The shield aids in learning as it helps in maintaining a closer distance with respect to the leader car. The dashed black line represents the minimum safety distance the ego robot should maintain to not violate the safety specification. Similarly, the bottom row shows the learning phase for the grid world scenario. Again, we observe that the shield aids in the learning phase, as the agent reaches closer to the optimal return very early when compared to the unshielded case.

respect to the required safety specification. Else, the shield does not modify the agent’s selected action.

Fig. 9 shows the learning curve for RL agents that learn to navigate in the grid world environment and the car-following scenarios in our simulations section. For the grid world environment, we show how a tabular Q-learning approach learns to maximize the episode return over time. Similarly, for the car-following scenario, where the objective is to cover as much distance as possible without colliding with the leader car, we show how a deep RL agent learns to be as close as possible to the leader car and not collide, using the Soft Actor Critic algorithm. Clearly, in the presence of delay, the RL agent with shield learns faster than the RL agent without shield. Additionally, with the shield, we observe that safety is ensured *during* training for networked control systems.

E. Experiment Parameters

In this section, we describe the environments’ design choices used to validate our safe networked control approach.

We also explain the off-the-shelf controllers used in our environments.

Car-following: In the simulations for car-following, we assume that at any time step, the leader car can accelerate between $-0.5m/s^2$ and $0.5m/s^2$. Similarly, the bounds on ego robot acceleration are set to $-1m/s^2$ and $1m/s^2$. We construct a discrete MDP using finite state-action abstraction on our continuous MDP. The discrete states for s_{rel} are $[-\infty, 1m]$, $[1m, 2m]$, ..., $[25m, \infty]$, and the discrete states for v_{rel} are $[-\infty, -5m/s]$, $[-5m/s, -4m/s]$, ..., $[4m/s, 5m/s]$, $[5m/s, \infty]$. We consider 5 discrete actions, $a_{ego} \in [-1, -0.5, 0, 0.5, 1]$. For our off-the-shelf controller, we used a model-free deep RL approach trained to maximize distance travelled and minimize the risk of collision. We use Soft Actor Critic algorithm to train our deep RL agent. Our actor is a simple feedforward neural network with 3 layers with 256 units in each layer. Similarly, our critic is also a simple feedforward neural network with 3 layers with 256

units in each layer. We consider episodes of length 100 steps and at each step, the reward is the distance travelled by the ego-robot. If, at any step, the ego-robot collides with the leader car, the environment provides a negative reward of -10 . We convert the continuous action output from the actor network to the discrete action by mapping the action output to the nearest next action from $[-1, -0.5, 0, 0.5, 1]$.

Grid World: For the grid world environment, we use a tabular Q-learning approach to learn our off-the-shelf controller. At each time step, we provide a negative reward of -10 for collision, and, if the robot moves towards the goal, it receives a positive reward. Additionally, if the robot reaches the goal before the episode terminates, it receives a reward of 2.

Real world demonstration: For our real world demonstration, we use F1/10th cars. The abstraction follows the car-following environment. Our setup works as follows, the laser scan with 1080 range measurements is sent to a remote server over a stochastic WiFi link. Along the robot's direction of motion, we find if there are any laser scan readings, which corresponds to the leader car. The corresponding range measurement gives the distance from the leader car which is denoted by s_{rel} . This is provided to a time-optimal controller (off-the-shelf controller) to compute the action that the ego robot should execute.